CORA Cork Open Research Archive
Cartlann Taighde Oscailte Chorcaí

Title	Dipole lasing phase transitions in media with singularities in polarizabilities
Authors	Protsenko, I. E.;O'Reilly, Eoin P.
Publication date	2006
Original Citation	Protsenko, I. E. and O'Reilly, E. P. (2006) 'Dipole lasing phase transitions in media with singularities in polarizabilities', Physical Review A, 74(3), 033815 (10pp). doi: 10.1103/PhysRevA.74.033815
Type of publication	Article (peer-reviewed)
Link to publisher's version	https://journals.aps.org/pra/abstract/10.1103/PhysRevA.74.033815 - 10.1103/PhysRevA.74.033815
Rights	© 2006, American Physical Society
Download date	2026-11-17 12:47:01
Item downloaded from	https://hdl.handle.net/10468/4553



UCC
University College Cork, Ireland
Coláiste na hOllscoile Corcaigh

Dipole lasing phase transitions in media with singularities in polarizabilities

I. E. Protsenko[1,2] and E. P. O'Reilly[2]
[1]*Lebedev Physical Institute, Leninsky Prospect 53, Moscow, Russia*
[2]*Tyndall National Institute, Lee Maltings, Cork, Ireland*
(Received 14 June 2006; published 20 September 2006)

We show that a divergence in the optical polarizability of a heterogeneous medium with nonlinear amplification and a strong dipole-dipole interaction between particles can lead to a phase transition, for which the dipole momentum of the particles or the dipole radiation rate can be taken as order parameters. The "dipole laser" [Phys. Rev. A **71**, 063812 (2005)] can be used both as a simple example of such a second-order phase transition and to provide a recipe for its analysis. We show that similar phase transitions may be possible for a nanoparticle on the surface of an optically active medium and at the "Clausius-Mossotti" catastrophe in a bulk heterogeneous medium.

DOI: 10.1103/PhysRevA.74.033815 PACS number(s): 42.55.Ah, 42.70.Nq, 42.70.Hj

I. INTRODUCTION

The enhancement of the local electromagnetic field near nanostructures gives rise to many novel and interesting phenomena in optics. These include surface-enhanced Raman scattering (SERS) [1] and enhanced fluorescence [2] near nanoparticles, an increase of the refractive index in a thin film due to nanocrystals [3], plasmon resonance narrowing [4], and "hot spots" localized on rough surfaces [5] and in engineered nanostructures [5(b)], all of which have been experimentally realized. Such enhanced local fields are now attracting high interest for practical application in areas such as biosensing [6], near-field microscopy [7,8], and highly efficient photocurrent generation [9,10]. Many of these phenomena and their applications utilize plasmon resonances in metal objects, in which the objects are of subwavelength (nano) size in at least one dimension. Research into the optical and other properties of such objects has opened the field of plasmonics, involving modern optics, material physics, and chemistry [11]. Many interesting plasmonic phenomena are related to the modification of the resonant emission, absorption, or dispersion of light by localized plasmon resonances (LPR), as illustrated, for example, by SERS on nanoparticles [1] or enhanced fluorescence near nanobodies [2]. The physical mechanisms leading to the modification of the fluorescence may also, under certain conditions, result in lasing from individual nanostructures, as described in recent proposals for a dipole nanolaser (DNL) [12,13] and for surface plasmon amplification by stimulated emission of radiation (SPASER) [14].

The modification of the optical properties of a heterogeneous material due to a strong local field was first investigated theoretically a long time ago, including the possibility of a singularity ($\alpha \to \infty$) in the polarizability α of particles, which leads, for instance, to the so-called Clausius-Mossotti catastrophe [15]. However, the physical nature of these singularities and the optical properties of media as $\alpha \to \infty$ are still not well understood, despite the wide interest in these questions [16–18]. It is not quite obvious even whether $\alpha \to \infty$ points to a physical phenomenon or whether it is just a consequence of approximations made in the theoretical models. The recent experimental and engineering achievements in plasmonics now require a theory which is able both to predict and optimize the advanced properties of plasmonic devices in the presence of strong local fields, in order to take full advantage of regimes where $\alpha \to \infty$.

The purpose of this paper is to show that individual nano-objects or bulk media may, as $\alpha \to \infty$, have optical properties similar to a DNL [13]; to demonstrate these properties by use of specific examples; and to formulate a general theoretical approach for modeling the optical properties of heterogeneous media in the case where $\alpha \to \infty$.

A brief description of the local field in the model of Refs. [15,19] is first presented in Sec. II followed by an example from this model of $\alpha \to \infty$, in order to deduce the general conditions required for $\alpha \to \infty$. Section III focuses on the dipole nanolaser, showing that $\alpha \to \infty$ in a DNL [13] corresponds to the "dipole lasing" threshold, which can be described in terms of a second-order phase transition when the dipole momentum or the radiation rate of the DNL are considered as order parameters. Some properties of the DNL phase transition in an external field are also found and discussed. Section IV considers a metal particle on an active substrate as a nanoemitter, with a phase transition similar to the DNL as $\alpha \to \infty$. Section V generalizes the analysis of the DNL phase transitions developed in Secs. III and IV to the case of the bulk active heterogeneous medium with $\alpha \to \infty$ introduced in Section II. Finally, the results are discussed and summarized in the conclusion.

II. SINGULARITY IN POLARIZABILITY DUE TO A LOCAL FIELD

The local field (LF) plays an important role in the phenomena discussed below. A brief description of its physical nature and a simple model of the LF are given here; more details can be found in many papers [20–24] and books [15,25]. A monochromatic electromagnetic field $\vec{E}_{act}$ in a medium can be separated into two parts,

$$\vec{E}_{act} = \vec{E} + \vec{E}_{loc}, \tag{1}$$

where $\vec{E}$ is a solution of the macroscopic Maxwell equations [25], referred to as the "Maxwell" field, and $\vec{E}_{loc}$ is the local

 ©2006 The American Physical Society

field. $\vec{E}_{loc}$ includes all modes of radiation different from the modes of $\vec{E}$. Both $\vec{E}_{loc}$ and $\vec{E}$ can be described in terms of the superposition of dipole radiation from the individual particles composing the medium. In a macroscopic medium, dipole radiation modes, apart from the modes of $\vec{E}$, cancel each other due to destructive interference everywhere, except in a volume $\sim(\lambda/2\pi)^3$ near to a (dipole) particle, where λ here is the wavelength of the applied field. The greater the probability to find two or more particles in the volume $\leqslant(\lambda/2\pi)^3$, the larger the contribution of $\vec{E}_{loc}$ to $\vec{E}_{act}$.

In order to describe the optical properties of a macroscopic medium, one has to take the macroscopic polarization $\vec{P}$ of the medium as a source both for $\vec{E}$ and for $\vec{E}_{loc}$. $\vec{E}$ is related to $\vec{P}$ through the macroscopic Maxwell equations. The contribution of $\vec{E}_{loc}$ is significant only in a small volume $[\leqslant(\lambda/2\pi)^3]$ near to a dipole, so that as a first approximation one can ignore spatial and temporal dispersion and assume an instant and local relation between $\vec{E}_{loc}$ and $\vec{P}$, by taking $\vec{E}_{loc}=\vec{E}_{loc}(\vec{P})$. By expanding this relation in a series we have

$$\vec{E}_{loc}(\vec{P}) = 4\pi\overleftrightarrow{C}\vec{P} + \cdots, \tag{2}$$

where $\overleftrightarrow{C}$ is, in general, a tensor [20]. Corrections to Eq. (2) arise from multipole interactions, from any anisotropy and ordered structuring in the medium [20], and from self-broadening [21]. In the case of a uniform homogeneous medium of randomly distributed dipoles $\overleftrightarrow{C}=C_L=1/3$, as derived in Ref. [19] and later verified by calculations involving explicit dipole-dipole interactions (see, for example, Refs. [20,22]). An expansion of $\vec{E}_{loc}$ similar to Eq. (2) can be found in the theory of ferroelectric media in a constant electric field [26,27].

In principle, the Maxwell field $\vec{E}$ has to be replaced everywhere in this theory by the field $\vec{E}_{act}$ given in Eqs. (1) and (2) [20,24]. Several predictions have been made based on the contribution of the LF in coherent media, including for example bistability in a gas of two-level atoms [22] or an enhancement of the index of refraction associated with electromagnetically induced transparency (EIT) [24]. In practice, however, the LF disrupts the coherency of the interaction of the dipoles with light causing, for example, self-broadening [28]. A nondestructive participation of the LF in coherent phenomena can be seen for nanoscaled objects under specific conditions, such as SERS on gold particles [1], and fluorescence enhancement [2] or spontaneous emission enhancement near to nanobodies [8]. A singularity in the polarizability α of individual particles can also provide the condition for many unusual phenomena associated with the LF [16,18].

The best-known example of $\alpha\to\infty$ is found in the Clausius-Mossotti theory of the dielectric function [15]. Suppose that a medium consists of $n+1$ kinds of homogeneously distributed dipoles d_i, $i=0\ldots n$. Applying Eqs. (1) and (2), we have $d_i=\alpha_i E_{act}=\alpha_i^{act}E$, where $\alpha_i=\alpha_i'+i\alpha_i''$ and α_i^{act} are the polarizabilities of a solitary dipole and of the dipole in the heterogeneous medium, respectively. We can relate these polarizabilities to each other as

$$\alpha_i^{act} = \frac{\alpha_i}{1 - 4\pi C_L \sum_{j=0}^{n} \alpha_j N_j}, \tag{3}$$

where N_j is the volume concentration of dipoles d_j. Equation (3) provides an approximate relation, because it is derived from the approximate expression (2). In the case of a perfectly transparent heterogeneous medium where

$$\sum_{j=0}^{n} \alpha_j'' N_j = 0, \tag{4a}$$

Eq. (3) predicts that $\alpha_i^{act}\to\infty$ when

$$\sum_{j=0}^{n} \alpha_j' N_j = \frac{1}{4\pi C_L}. \tag{4b}$$

Is this singularity a consequence of approximations made in the derivation of Eqs. (2) and (3), or does it correspond to a physical phenomenon similar to the ferroelectric phase transition [26]? To find the answer to this question, the divergence $\alpha_i^{act}\to\infty$ predicted by Eq. (4) and the divergence in the polarizability of a dipole nanolaser [12,13] will be compared in Sec. V.

Let us suppose for a moment that $\alpha_i^{act}\to\infty$ has physical sense and discuss what kind of medium we need to achieve $\alpha_i^{act}\to\infty$. We note that $\alpha_i^{act}\to\infty$ can be hardly realized in a transparent dielectric nonresonant medium [15]. We suppose, for simplicity, that such a medium contains only one kind of dipole, which we describe by spherical dielectric particles, so that

$$\alpha_{act} = \alpha/(1 - 4\pi C_L N_0 \alpha), \tag{5}$$

for which we can achieve $\alpha_{act}\to\infty$ as $N_0\to N_{cr}=(4\pi C_L\alpha)^{-1}$. For spherical dielectric particles $\alpha<(3/4\pi)V$, where V is the volume of a particle [27], to reach $\alpha_{act}\to\infty$ one needs a concentration of particles per unit volume of $\eta\equiv VN_0>1$, which is impossible. In general, the condition (4b) can be interpreted as requiring an "overlap" in the polarizabilities of neighboring particles, which only becomes possible when $|\alpha|>V$.

The condition $|\alpha|>V$ and even $|\alpha|\ll V$ can be realized for the resonant interaction of a particle with an electromagnetic field. For example, the polarizability $|\alpha|$ of a two-level atom in a vacuum approaches $(3/4)(\lambda/2\pi)^3$ when in resonance with an electromagnetic field of wavelength λ. The excitation of a localized plasmon resonance (LPR) [27] in a metal nanoparticle provides another example where $|\alpha|>V$.

Suppose in Eq. (5) that $\alpha=\alpha\prime+i\alpha''$, where $\alpha''>0$ and define $a\equiv\alpha''/\alpha'$, with $|a|\ll 1$, which implies small absorption and which is in general true for the polarizability α of a metal nanoparticle. Let us now examine the possibility for high dispersion due to the local field $(\alpha_{act}'/\alpha'\ll 1)$ in a resonant heterogeneous medium containing nanoparticles where we have small absorption at the LPR, and where condition (4a) is approximately satisfied. By taking $N_0=N_{cr}(1-\Delta)$ with $|\Delta|\ll 1$, we obtain from Eq. (5) as we approach $N_{cr}\cong(4\pi C_L\alpha')^{-1}$ that

$$\frac{\alpha_{act}}{\alpha\prime} = \frac{\Delta - a^2}{\Delta^2 + a^2} + i\frac{a}{\Delta^2 + a^2} \approx \frac{1}{\Delta} + i\frac{a}{\Delta^2}, \tag{6}$$

where the approximation is made of assuming $a \ll |\Delta| \ll 1$. Thus the increase in $\alpha_{act}{}'$ of $1/\Delta \gg 1$ is accompanied by an increase in the absorption $\sim 1/\Delta^2$. Estimates made for silver and gold metal particles show that such an increase in the absorption makes it difficult to take practical advantage of the enhancement in $\alpha_{act}{}'$ in a passive heterogeneous medium with an LPR. Nevertheless, there are very interesting theoretical results on LPR narrowing (i.e., an increased LPR quality factor, which means, effectively, a reduction in absorption), which have also been observed experimentally [4] in ordered (linear) structures of nanoparticles, and which may go some way towards overcoming this difficulty.

In addition, the possibility of $\alpha_{act} \to \infty$ may exist in resonant active heterogeneous media, where absorption in the metal nanoparticles at the LPR is compensated by optical gain due to some active components, such as impurity ions or semiconductor microcrystals. The concentration of these components must be such that conditions (4a) and (4b) are satisfied.

The idea of absorption compensation in a resonant medium with metal nanoparticles due to inclusion of an active gain component was suggested in Refs. [16,17]. Individual metal nanoparticles in a medium with optical amplification were considered in Ref. [18], and singularities in the polarizability have been related to random laser action [29]. In Refs. [16–18], the amplification coefficient necessary for absorption compensation was estimated as $\sim 10^3 - 10^4$ cm^{-1}, which is achievable in modern dye or semiconductor materials. Media with high polarizabilities and absorption compensation due to EIT were proposed in Ref. [24]. In the next section, we discuss the interpretation of singularities in the polarizability for the case of the dipole nanolaser proposed in Refs. [12,13].

III. POLARIZABILITY SINGULARITIES, PHASE TRANSITIONS, AND MULTISTABILITY IN A DIPOLE NANOLASER

A dipole nanolaser, composed of a metal nanoparticle and a two-level system with population inversion (Fig. 1) provides a simple example for the analysis and interpretation of singularities in the polarizability.

Let us consider the interaction of a DNL with a monochromatic external field of amplitude E, frequency ω, and wavelength λ. By inserting terms $-\mu_0(a_0^+ E + E^* a_0)$ and $-\mu_2(\sigma^+ E + E^* \sigma)$ into the Hamiltonian H of Ref. [13], one comes to a set of equations for the DNL in an external field,

$$\dot{D} = 2i\left[\Omega_{\text{int}}(a_0^+\sigma - \sigma^+ a_0) + \frac{\mu_2}{\hbar}(a_0 E^* - E a_0^+)\right] - \frac{1}{\tau}(D - D_0), \tag{7}$$

$$\dot{\sigma} = (i\delta_2 - \Gamma_2)\sigma + i\left(\Omega_{\text{int}} a_0 - \frac{\mu_2 E}{\hbar}\right)D, \tag{8}$$

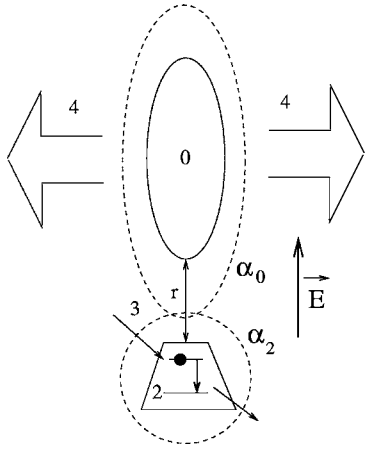


FIG. 1. Schematic of a dipole nanolaser (DNL). The metal nanoparticle 0 is separated from the two-level system 2 by a distance r such that the polarizabilities α_0 and α_2 of the particles overlap each other. The pump 3 creates a population inversion in the two-level system. The dipole momentum of the particle appears spontaneously when the conditions (11b) are satisfied. The particle then emits coherent dipole radiation 4. The DNL may also interact with an external monochromatic electromagnetic field E.

$$\dot{a}_0 = (i\delta_0 - \Gamma_0)a_0 + i\left(\frac{\mu_0 E}{\hbar} - \Omega_{\text{int}}\sigma\right), \tag{9}$$

where D is the population inversion of the two-level active particle; $\mu_0 a_0$ and $\mu_2 \sigma$ are the dipole momentum of the metal nanoparticle and the two-level particle, respectively; $\delta_2 = \omega - \omega_2 \ll \omega$ and $\delta_0 = \omega - \omega_0 \ll \omega$ are the detuning of the applied field frequency from the two-level transition frequency ω_2 and the frequency ω_0 of the LPR of the metal particle; $1/\tau$, Γ_2, and Γ_0 are relaxation rates; D_0 is the normalized pump rate of the two-level particle; $\Omega_{\text{int}} = \xi\mu_0\mu_2/r^3$ is the dipole-dipole interaction of the metal and two-level particle with each other; $r \ll \lambda/(2\pi)$ is the distance between the particles; and the factor $\xi \sim 1$ depends on the mutual orientation of the particles (for more details, see Ref. [13]). The decay rate $\tau^{-1} = \tau_d^{-1} + \tau_p^{-1}$, where $\tau_{d,p}^{-1}$ are, respectively, the damping and the pump rates in the two-level system. It is supposed in Eqs. (7)–(9) that $r \ll \lambda/(2\pi)$, so that the phase of E is the same at particles 0 and 2.

From the stationary solution of Eqs. (7)–(9), one can find the polarizability $\alpha_{tot} = (\mu_0 a + \mu_2 \sigma)/E$ of the two particles,

$$\alpha_{\text{tot}} = \alpha_0 b_0 - (\alpha_2 D) b_2, \tag{9a}$$

in terms of the nonsaturated polarizabilities α_0 and α_2, and the polarizability enhancement factors b_0 and b_2 for the metal nanoparticle and two-level particle, respectively. (Note that the "-" sign in Eq. (9a) arises because D is defined as the population inversion.) Here,

$$\alpha_i = \frac{\alpha_{ir}}{\Delta_i - i}, \quad \alpha_{ir} = \frac{\mu_i^2}{\hbar\Gamma_i}, \quad \Delta_i = -\frac{\delta_i}{\Gamma_i}, \quad i = 0,2,$$

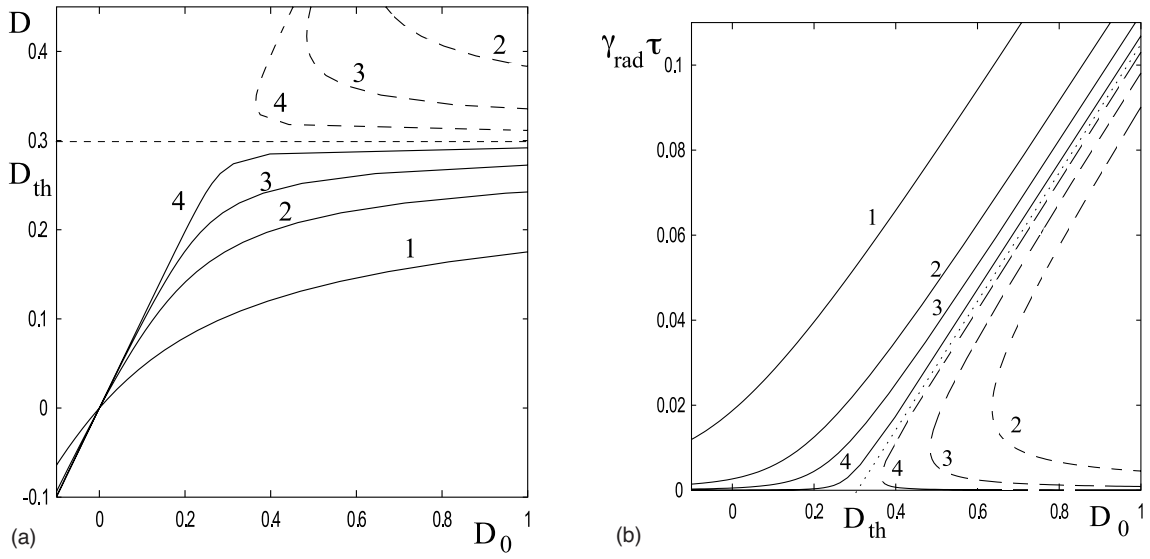


FIG. 2. (a) Normalized gain (population inversion D) of the two-level system in the DNL and (b) DNL radiation rate versus the normalized pump rate for various intensities of external field taken in units of saturated intensity for the two-level system, with $I=0.7$ (curves 1), 0.1 (2), 0.02 (3), 0.001 (4). The dashed curves correspond to unstable stationary solutions with $D>D_{th}$.

$$b_0(D) = \frac{1+\xi\alpha_2/r^3}{1+\xi^2(\alpha_2\alpha_0/r^6)D}, \quad b_2(D) = \frac{1-\xi\alpha_0/r^3}{1+\xi^2(\alpha_2\alpha_0/r^6)D}. \tag{10}$$

The population inversion D can be found from the implicit equation

$$D \equiv D[|b_2(D)|^2 I] = \frac{D_0}{1+|b_2(D)|^2 I}, \tag{11}$$

where $I=|E|^2/E_s^2$ and $E_s^2=\hbar/(4\tau \operatorname{Im}\alpha_2)$ is the saturation energy density of the external field for the two-level particle, and

$$D(I) = D_0/(1+I) \tag{11a}$$

is the normalized amplification coefficient of the two-level system. Equation (11) shows that b_2 is also the enhancement factor for the field near the two-level particle, i.e., the field near the particle is $E_{act}=b_2E$.

Equations (9a) and (10) predict a singularity in α_{tot}. Indeed, $\alpha_{tot}\to\infty$ if $|E|^2\to 0$ and

$$D_0 = D_{th} \equiv r^6/(\xi^2\alpha_0\alpha_2), \quad \Delta_0 = -\Delta_2 \equiv \Delta, \tag{11b}$$

which are precisely the conditions for dipole lasing found in Ref. [13]. This means that the divergence in α_{tot} corresponds to the spontaneous generation of dipole momentum, which happens in the DNL when Eq. (11b) is satisfied. The singularity $\alpha_{tot}\to\infty$ disappears at small, but finite E. When no external field is applied, this small E can be attributed to thermal or other noise; a detailed analysis of the DNL with noise will be carried out elsewhere using, for example, the approach of Ref. [30].

Neither the polarizability nor the dielectric function is a directly observable quantity. One can see from Eqs. (10) and (11) that observable quantities in the DNL such as, for example, the dipole momentum $\alpha_{tot}E$ or the dipole radiation rate $\gamma_{rad}\sim|\alpha_{tot}E|^2$, do not have singularities. One can find from Eqs. (10) and (11) that

$$\gamma_{rad} = \frac{4k^3}{3\hbar}|\alpha_{\mathrm{tot}}E|^2, \quad |\alpha_{\mathrm{tot}}E|^2 = \frac{|\alpha_0-\alpha_2 D+\xi(\alpha_2\alpha_0/r^3)(D+1)|^2}{|1-\xi\alpha_0/r^3|^2}E_s^2 I_D(D), \tag{12}$$

where $I_D(D)=(D_0/D)-1$ is the inverse of the amplification coefficient function of Eq. (11a) and $D(D_0)$ is determined from Eq. (11). We see from Eqs. (11) and (12) that γ_{rad} does not experience a singularity, despite the divergence in α_{tot}. This is similar to what is found for a linear Fabry-Pérot amplifier at lasing threshold, where the singularity in the amplification coefficient does not lead to a singularity in the lasing field [31]. Figures 2(a) and 2(b) display $D(D_0)$ and $\gamma_{tot}(D_0)$ for various values of the incident intensity I and with the DNL parameters chosen as in Ref. [13].

When $I\to 0$ and the pump rate exceeds the DNL threshold, $D_0>D_{th}=0.3$, then population clamping occurs, with the population inversion D remaining close to D_{th}. For $D_0<D_{th}$ the population inversion approaches the pump rate $D\cong D_0$, see Fig. 2(a). As $I\to 0$, the radiation rate $\gamma_{rad}(D_0)$ remains close to 0 for $D_0<D_{th}$ and increases linearly with D_0 at $D_0>D_{th}$, Fig. 2(b). This variation of the amplification and of the order parameter (lasing mode intensity) with pump intensity is typical of a lasing phase transition [32]. The curves for $I\neq 0$ in Fig. 2 resemble a thresholdless laser [30].

Thus, $\alpha_{tot}\to\infty$ describes in this case a second-order phase transition, with the radiation rate γ_{rad} as the order parameter and the pump rate D_0 as the control parameter. An external field with intensity $I\neq 0$ eliminates the breakdown in the derivatives dD/dD_0 and $d\gamma_{rad}/dD_0$ at the second-order phase transition at $D_0=D_{th}$, similar to the influence of noise near to threshold in lasers [30]. As the external field increases, the

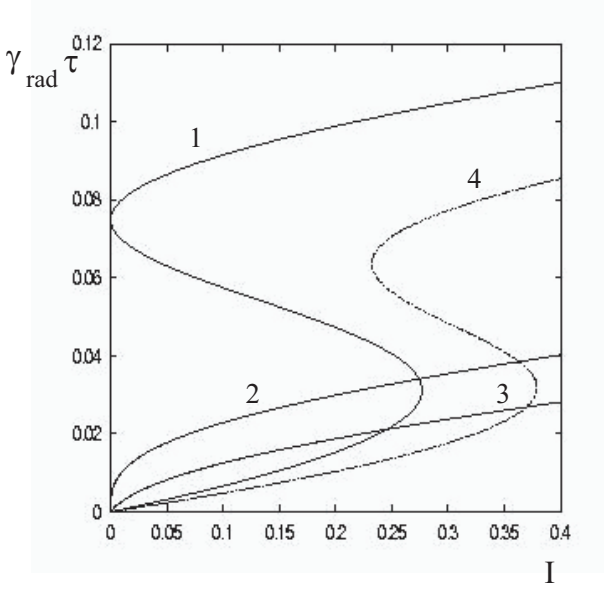


FIG. 3. (Color online) Radiation rate of a DNL in an external field above the DNL threshold, Curve (1): $D_0=0.8>D_{th}=0.3$, (2): at threshold; (3): below threshold with $D_0=0.2$, and (4) when the dipole lasing conditions are not satisfied ($D_0=0.8$ but $\Delta_0=\Delta_2=0.2$).

distortion disappears in the $D(D_0)$ and $\gamma_{rad}(D_0)$ curves near to $D_0=D_{th}$ (curves 1–3 in Fig. 2). The dashed curves in Fig. 2 correspond to the stationary solutions of Eqs. (7)–(9) with $D>D_{th}$. Such solutions are also found in conventional lasers [30], where they are also unstable.

A first-order phase transition can be observed in the DNL, when I is chosen as a control parameter (see Fig. 3). Hysteresis and jumps in γ_{rad} can be observed when I approaches critical values where $d\gamma_{rad}/dI\to\infty$.

A first-order phase transition can occur even if the conditions for dipole lasing are not satisfied (curve 4 in Fig. 3). The region of the DNL parameter space in which a first-order phase transition is possible can be readily determined using the standard methods of catastrophe theory [33].

We conclude that a singularity in the polarizability of a DNL is associated with a phase transition, for which the DNL dipole momentum or radiation rate can be used as order parameters. The DNL is a system with a strong local field which provides, through the dipole-dipole interaction, feedback between the two-level system and the metal nanoparticle. Let us now investigate divergences in the polarizability of other systems with a local field and optical gain. The example of the DNL (i) provides a method to take account of gain saturation (as was also reported in Ref. [18]); and shows that (ii) the radiation rate or the dipole momentum should be chosen as order parameters, because they do not have singularities; (iii) the optical gain can be used as a governing parameter to find the second-order "DNL-like" phase transition; and (iv) the external field amplitude can be used as a control parameter in a first-order phase transition. In general, one does not need to derive dynamical equations such as Eqs. (7)–(9) for each system under consideration; it is sufficient to examine the effective polarization due to the local field.

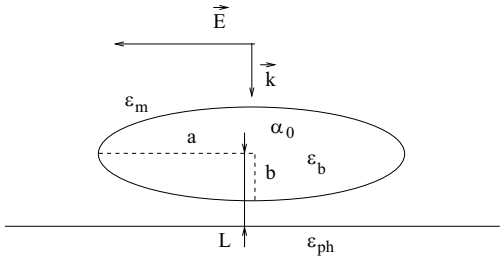


FIG. 4. Ellipsoidal particle with semiaxes a and b on the surface of an active medium.

IV. DIPOLE LASING FROM A NANOPARTICLE ON THE SURFACE OF AN ACTIVE MEDIUM

The polarizability α_{eff} of a nanoparticle near to a planar interface between two media (see Fig. 4) is given by Ref. [34],

$$\alpha_{eff}=\alpha_0 b_0,\quad b_0=\frac{1+\xi}{1+A\xi},\quad A\equiv\alpha_0 p/(2L)^3 \tag{13}$$

where b_0 is the polarizability enhancement factor, L is the distance from the center of the nanoparticle to the interface, the factor p depends on the orientation of the polarization of the external field with respect to the interface, with $p=1$ for the case shown in Fig. 4;

$$\xi=\frac{1-\varepsilon_{eff}}{1+\varepsilon_{eff}}, \tag{14}$$

where $\varepsilon_{eff}=\varepsilon_{ph}/\varepsilon_m$, and ε_m and ε_{ph} are the dielectric function of the medium holding the nanoparticle and below the interface, respectively. Equation (13) takes into account the interaction of the particle with the medium below the interface through the near (dipole) field. Equation (13) is derived using a quasistatic approximation, where the size of the particle is much smaller then λ and where we also neglect the reflection of the electromagnetic field from the interface, which is a good approximation if $\varepsilon_m'\approx\varepsilon_{ph}'$ and $|\varepsilon_{ph}''|\ll|\varepsilon_{ph}'|$.

We suppose that $\varepsilon_m\equiv n_m^2$ is real, and that the medium below the interface is optically active, i.e.,

$$\varepsilon_{ph}\cong n_{ph}^2-i\kappa n_{ph}/k, \tag{14a}$$

where $\kappa>0$ is the amplification coefficient, n_{ph} is the refractive index, $k=2\pi/\lambda$, and $\kappa/k\ll n_{ph}$. It follows from Eq. (13) that $b_0\to\infty$, and therefore $\alpha_{eff}\to\infty$, if $\mathrm{Im}(A\xi)=0$ and $\mathrm{Re}(A\xi)=-1$. This occurs when

$$\frac{|A|^2-1}{|A-1|^2}=\left(\frac{n_{ph}}{n_m}\right)^2,\quad \kappa\to\kappa_{th}\equiv kn_{ph}\frac{2A''}{|A|^2-1}. \tag{15}$$

The first of the conditions in Eq. (15) for $A\sim\alpha_0=\alpha_0(\lambda)$ determines the wavelength at which $\alpha_{eff}\to\infty$. A necessary condition for $\alpha_{eff}\to\infty$ is that $|A|>1$ or $L<(\alpha_0 p)^{1/3}/2$, which can be satisfied at the LPR, when α_0 exceeds the geometrical size of the nanoparticle. The conditions given by Eq. (15) can be fulfilled, for example, for an ellipsoidal silver nanoparticle with polarizability

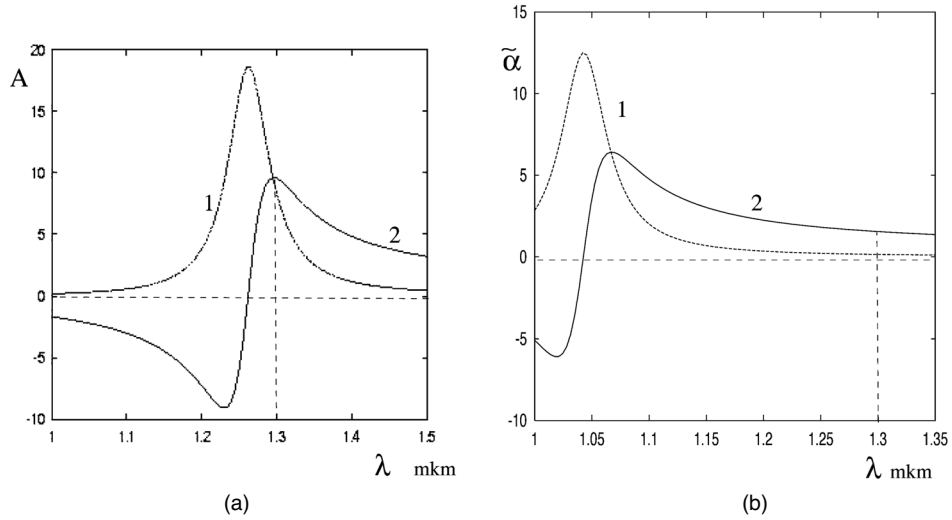


FIG. 5. (a) Imaginary (curve 1) and real (curve 2) parts of $A \sim \alpha_0$ given by Eqs. (13) and (15a) for the parameter values indicated in Sec. IV. The minimum value of κ_{th} is achieved when the wavelength of maximum amplification in the substrate corresponds to the maximum of A' at $\lambda = 1.3$ μm. (b) Real (1) and imaginary (2) parts of the normalized polarizability of the silver nanoparticle in a bulk heterogeneous medium [see Eq. (15a)]. The vertical dashed lines indicate the wavelength where maximum amplification is required.

$$\alpha_0 = \frac{V}{4\pi}\tilde{\alpha}, \quad \tilde{\alpha} = \frac{\varepsilon_b/\varepsilon_m - 1}{1 + n(\varepsilon_b/\varepsilon_m - 1)}, \tag{15a}$$

where ε_b is the dielectric function of bulk silver, V is the nanoparticle volume and $0 < n < 1$ is a depolarizability factor, which depends on the shape of the particle. Let us consider an ellipsoidal silver nanoparticle with $n = 0.1$ (for which the aspect ratio of the nanoparticle axes $a/b \approx 3$), and with $\varepsilon_b(\lambda)$ taken from Ref. [35]. The nanoparticle is in a medium with $n_m = 3$ at a distance $0.1b$ above the semiconductor substrate, and with $n_{ph} = 3.17$; see Fig. 4. One can show that $\kappa_{th} \approx 1.6 \times 10^3$ cm^{-1} at $\lambda = 1.3$ μm, which is of the order of amplification coefficient available in semiconductor laser materials. The wavelength $\lambda = 1.3$ μm corresponds to the maximum in the dispersion curve near to the LPR, see Fig. 5(a).

One can show that $\alpha_{eff} \to \infty$ corresponds to a phase transition similar to that predicted for the DNL in Sec. III. The amplification coefficient depends on the local field $\kappa = \kappa(I_{act})$, where $I_{act} = |E_{act}|^2/E_s^2$ and E_s is the amplitude of the saturating field in the active medium below the interface. In order to understand how E_{act} is related to the applied field E, one has to refer to the procedure for the derivation of Eq. (13) [27]. In this procedure, the particle near the interface is replaced by a particle in a homogeneous medium with dielectric function ε_m and a new polarizability α_{eff} given by Eq. (13), i.e., it becomes an optically active nanoparticle in a homogeneous passive medium. Therefore, $E_{act} = E_{in}$, where E_{in} is the field inside the particle with polarizability α_{eff}. In accordance with Ref. [27], the field amplitude E_{in} inside that particle is

$$E_{in} = \frac{E}{1 + n(\tilde{\varepsilon}_b/\varepsilon_m - 1)}, \tag{16}$$

where $\tilde{\varepsilon}_b$ takes account of the interface and has to be determined from the relation $\alpha_0 b_0 = \alpha_{eff}$. Combining this last relation with Eqs. (15a) and (16), one can find

$$E_{in} = b_f E, \quad b_f = \frac{1 + n(1 - b_0)(\varepsilon_b/\varepsilon_m - 1)}{1 + n(\varepsilon_b/\varepsilon_m - 1)}, \tag{17}$$

where b_f is the enhancement factor for the field inside the particle. Now one can write an implicit expression for the amplification coefficient $\kappa(E_{in})$ of the active medium, which has to be substituted, through Eqs. (13) and (14a), into the expression for α_{eff},

$$\kappa = \kappa(|b_f(\kappa)|^2 I), \tag{18}$$

where $I = |E|^2/E_s^2$. Equation (18) is similar to Eq. (11) for the dimensionless amplification coefficient $D(E)$ of the DNL. The combination of Eqs. (13), (15a), (16), and (17) provides an expression for the radiation rate of a metal nanoparticle on the surface of an optically active medium,

$$\gamma_{rad}(\kappa) \equiv \frac{4k^3}{3\hbar}|\alpha_{eff}E|^2 = \gamma_0 \frac{|b_0(\kappa)|^2}{|b_f(\kappa)|^2} I_\kappa(\kappa), \tag{19}$$

where the coefficient $\gamma_0 = (4k^3|\alpha_0|^2 E_s^2)/3\hbar$ and $I_\kappa(\kappa)$ is the inverse of the function $\kappa(I)$. Equation (19) is similar to Eq. (12) for a DNL and shows that $\gamma_{rad}(\kappa)$ does not have a divergence, while the enhancement factors b_0 for the polarizability and b_f for the field both diverge. The amplification coefficient κ in Eq. (18) may be determined from experiment. Here we assume a simple saturation dependence of $\kappa(I)$

$$\kappa/\kappa_{th} = \Gamma_p/(1 + I), \tag{19a}$$

where the pump rate Γ_p is taken in units of the threshold pump rate Γ_{th}, so that $\kappa(I = 0, \Gamma_p = 1) = \kappa_{th}$. Equation (18) can be written, therefore, as $\Gamma_p = (\kappa/\kappa_{th})(1 + |b_f(\kappa)|^2 I)$, from which $\kappa(\Gamma_p)$ can be implicitly determined, in combination with Eqs. (13) and (17).

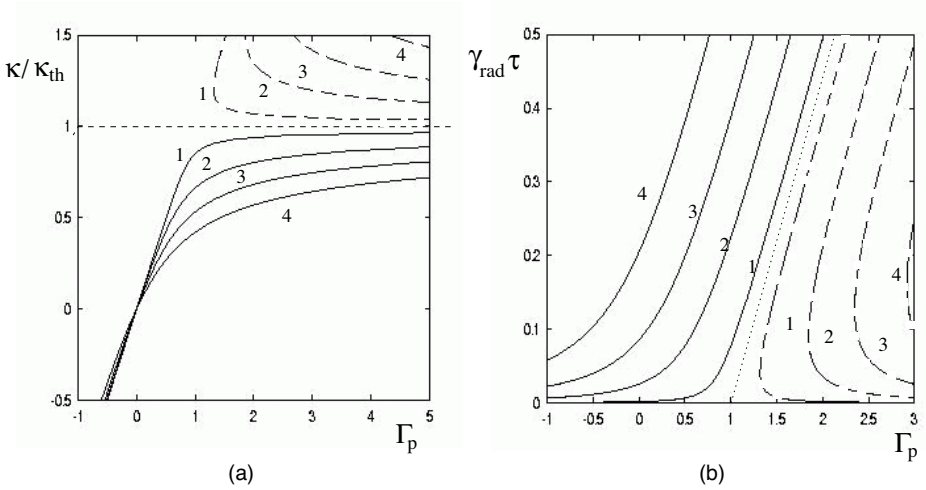


FIG. 6. (Color online) (a) Amplification coefficient in the substrate near a nanoparticle and (b) the radiation rate of the nanoparticle on the substrate as a function of the pump rate. Compare with Fig. 3. Curves 1–4 are for $I=10^{-5}$, 1.5×10^{-4}, 5×10^{-4} and 1.2×10^{-3}, respectively.

Figures 6(a) and 6(b) show the amplification coefficient κ of the active medium below the interface near the nanoparticle, and the radiation rate γ_{rad} of the nanoparticle respectively, both as a function of the pump rate Γ_p for various normalized intensities I of the external field. Similar to what was found for the DNL (Fig. 2), κ remains close to its threshold value κ_{th}, while γ_{rad} increases linearly with Γ_p, when $\Gamma_p > 1$ and $I \ll 1$. Thus a particle on the surface of an active medium can show a dipole lasing phase transition at $\kappa=\kappa_{th}$. Figure 7, which is similar to Fig. 3 for the DNL, displays $\gamma_{rad}(I)$ for various values of $\Gamma_p=\kappa/\kappa_{th}$, including above (curve 1), at (curve 2), and below the threshold value (curve 3), as well as in a case of a large Γ_p value, but where the conditions for dipole lasing are not satisfied (curve 4).

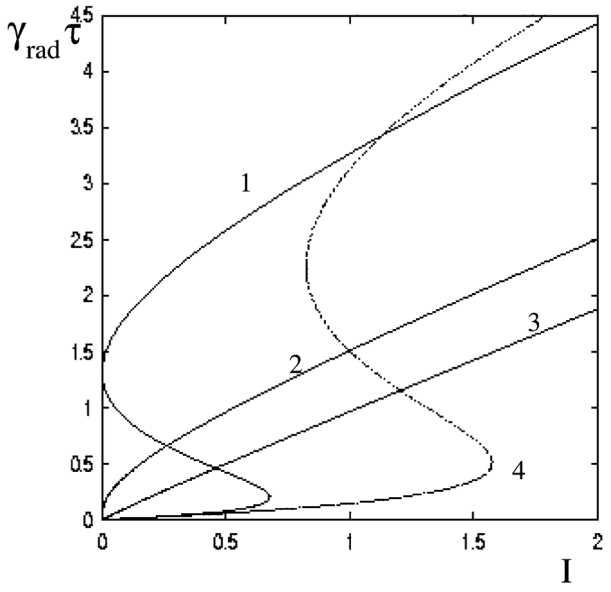


FIG. 7. Radiation rate from a silver nanoparticle on a substrate which provides optical gain, as a function of the normalized intensity of the external field for (curve 1): $\kappa/\kappa_{th}=4$, (2): 1; (3): 0.1; and (4): for $\kappa/\kappa_{th}=6$ but $n_m=3.1$, when the conditions for dipole lasing are not fulfilled.

V. DIPOLE LASING IN BULK MEDIA

The two preceding sections have analyzed singularities in the polarizability of an individual metal nanoparticle coupled with another active particle or with a bulk active medium through the near-field (dipole) interaction. A similar analysis can be applied for a bulk, optically active heterogeneous medium, which contains a homogeneous and random distribution of metal nanoparticles. The polarizability of the metal nanoparticles in this medium can be estimated from Eq. (4).

Let us consider a transparent dielectric matrix with refractive index n_m, which contains randomly distributed, but uniformly oriented, metal ellipsoidal nanoparticles and active light emitters, for example, rare earth ions. It is convenient to look for singularities in the dielectric function $\tilde{\varepsilon}_{het}$ of such a medium. From Eq. (4) one can obtain

$$\tilde{\varepsilon}_{het} = \frac{1+4\pi\tilde{\chi}_{het}(1-C_L)}{1-4\pi\tilde{\chi}_{het}C_L}, \tag{20}$$

where $\tilde{\chi}_{het}=\sum_i \alpha_i N_i$. Equation (20) is the Clausius-Mossotti relation [15]; it is approximate, and several versions of it can be found in the literature. For example, the Maxwell-Garnett formula derived in Ref. [36] can be obtained from Eq. (20), when the term $\alpha_m N_m$ related to the matrix medium is dropped from $\sum_i \alpha_i N_i$, while $\tilde{\varepsilon}_{het}$ is replaced by ε_{het}/n_m^2 and all the remaining polarizabilities α_i in $\sum_i \alpha_i N_i$ are calculated for particles in a matrix with refractive index n_m. The Maxwell-Garnet formula is convenient for our purposes. It is simple and can include the standard expressions for the polarizabilities of the nanoparticles in the dielectric matrix, as given by Eq. (15a). Other, more precise but complicated, expressions for $\tilde{\varepsilon}_{het}$ such as, for example, the Buggeman approximation

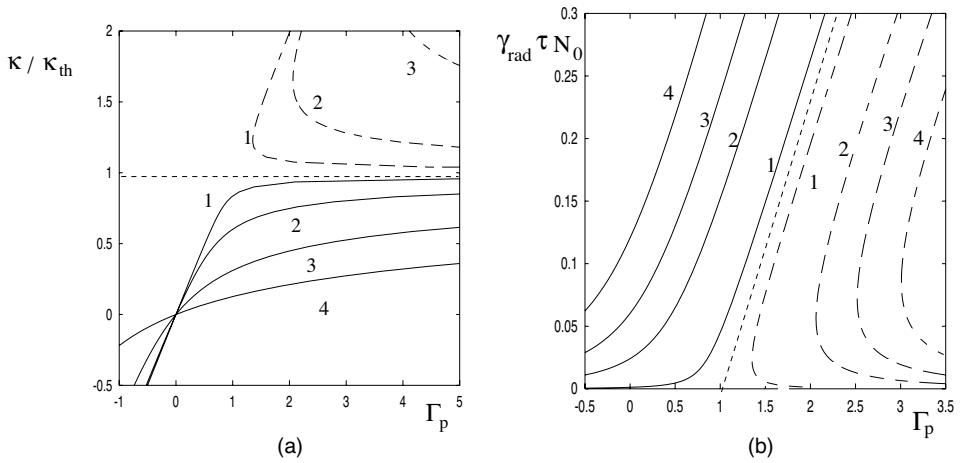


FIG. 8. (a) Normalized amplification coefficient and (b) the radiation rate per unit volume vs pump rate in a bulk heterogeneous active medium for four different values of the intensity of applied field normalized to the saturation intensity, namely $I=10^{-4}$ (curves 1), 2×10^{-3} (2), 2×10^{-2} (3) and 10^{-1} (4). The dashed curves correspond to unstable solutions. Compare with Figs. 2 and 6.

[37] can be analyzed in the same way as Eq. (20). We have in Eq. (20) that

$$4\pi\tilde{\chi}_{het} = \eta\tilde{\alpha} - i\kappa/k, \tag{21}$$

where $\eta=VN_0$ is the relative volume concentration of metal nanoparticles of volume V and concentration N_0; $\tilde{\alpha}$ is determined by Eq. (15a), κ is the amplification coefficient of the active particles in the matrix, and we neglect the contribution of the active particles to the dispersion. The condition $4\pi C_L\tilde{\chi}_{het}=1$ necessary to achieve the singularity $\varepsilon_{het}\to\infty$ [see Eq. (20)] is satisfied when

$$\eta = \eta_{cr} \equiv 1/[C_L\,\mathrm{Re}(\tilde{\alpha})], \quad \kappa = \kappa_{th} = k^{-1}\,\mathrm{Im}(\tilde{\alpha})/[C_L\,\mathrm{Re}(\tilde{\alpha})]. \tag{22}$$

For example, for $n_m=3.4$, with maximum amplification at $\lambda=1.3$ μm, $(k=2\pi/\lambda)$, and for ellipsoidal silver nanoparticles with axes aspect ratio $a/b=1.93$ and with $C_L=1/3$, one can find $\eta_{cr}=0.17$ and $\kappa_{th}=788$ cm^{-1}. The wavelength of maximum amplification is on the red side of the LPR, as shown in Fig. 5(b).

From Eqs. (1)–(3) and (20), with $\tilde{\varepsilon}_{het}=\varepsilon_{het}/n_m^2$ and using $P=4\pi\chi_{het}E$ and $\varepsilon_{het}=1+4\pi\chi_{het}$, one can obtain the field in the heterogeneous medium $E_{act}=b_f(\kappa)E$, where the field enhancement factor b_f is given by

$$b_f(\kappa) = 1 + \frac{C_L}{4\pi}\{\varepsilon_m[1 + b_0(\kappa)\tilde{\chi}_{het}(\kappa)] - 1\}, \tag{23}$$

$$b_0(\kappa) = \frac{1}{1 - C_L\tilde{\chi}_{het}(\kappa)},$$

and where b_0 is the polarizability enhancement factor [see Eq. (5)]. Using a saturation model of $\kappa(I,\Gamma_p)$ given by Eq. (19a), and using Eq. (18) with $b_f(\kappa)$ given by Eq. (23), one can find $\kappa(\Gamma_p)$ for various normalized intensities I of the external field; see Fig. 8(a). Similar to the cases of a DNL and of a metal particle on the surface of an active medium, the amplification saturates $(\kappa/\kappa_{th}\to1)$ as Γ_p increases above 1 at $\eta=\eta_{cr}$ and for $I\to0$.

By using Eq. (19), one can find the radiation rate γ_{rad} from a single metal nanoparticle. One has to insert $\alpha_{eff}=\alpha_0 b_0(\kappa)$ into Eq. (19), where the polarizability α_0 of an individual nanoparticle in the matrix is given by Eq. (15) and the polarizability enhancement factor $b_0(\kappa)$ is determined from Eq. (23). In the case of N_0 nanoparticles per unit volume, one can estimate the radiation rate per unit volume as $N_0\gamma_{rad}$ photons per second (neglecting any possible superradiance [38]). The variation of $N_0\gamma_{rad}$ as a function of κ is shown in Fig. 8(b) for various values of I. The way in which $\kappa(\Gamma_p)\to\kappa_{th}$ and the linear increase of $N_0\gamma_{rad}$ with Γ_p for $\Gamma_p>1$ displayed in Fig. 8 is very similar to the behavior observed in Figs. 2 and 6. We conclude that a "dipole lasing" phase transition can take place in a bulk heterogeneous active medium, when the conditions described by Eq. (22) are satisfied. Finally, Fig. 9 displays $\gamma_{rad}(I)$ at fixed Γ_p for parameter values above the DL threshold (curve 1), at threshold (curve 2), and below threshold (curve 3), and when $\eta=0.95\,\eta_{cr}$ so that the DL conditions of Eq. (22) are not satisfied (curve 4). $N_0\gamma_{rad}(I)$ displays multistability and a first-order phase transition, similar to that observed in Figs. 3 and 7.

VI. DISCUSSION AND CONCLUSIONS

We have shown that a metal nanoparticle on the surface of an active substrate and metal nanoparticles distributed throughout a bulk active medium can spontaneously display nonzero dipole momentum even in the absence of an external coherent field. This spontaneous dipole momentum arises through the second-order "dipole lasing" (DL) phase transition described in Ref. [13]. The DL radiation rate of the nanoparticles above the DL threshold increases linearly with the pump rate of the active medium. The amplification coefficient in the active medium saturates and remains close to its threshold value, similar to the behavior of the amplification coefficient of an ordinary laser. In contrast to the case of

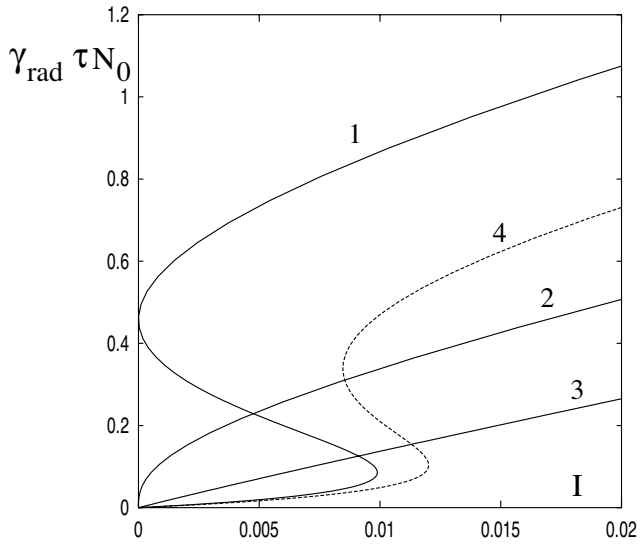


FIG. 9. The radiation rate per unit volume in a bulk active heterogeneous medium, as a function of the normalized intensity of the external field for (curve 1): $\eta=\eta_{th}$ and $\kappa/\kappa_{th}=3$, (2): 1, (3): 0.1, and (4): $\eta=0.95\eta_{th}$ and $\kappa/\kappa_{th}=3$. Compare with Figs. 3 and 7.

SERS or of fluorescence enhancement in media with metal nanoparticles, a population inversion is required in the light-emitting component of the heterogeneous medium in order to realize the DL regime. The spatial pattern of DL radiation is different from that of spontaneous emission, which is uniformly distributed over 4π solid angle in an isotropic medium. Above the DL phase transition, the dipole momentum of a nanoparticle acquires a specific polarization direction, and therefore radiates with a dipole radiation pattern. We propose that a structured array of many dipoles operating in the DL regime could produce nearly plane-wave coherent radiation, as occurs in the phased dipole arrays well-known from radio physics [39]. Well above the DL threshold, the coupling of dipoles through their coherent (far-field) radiation has to be taken into account, which will be the subject of future research. Another feature of DL is the narrowing of the radiation spectrum with increasing pump power above threshold, as is also well-known from conventional lasers. The radiation pattern and the linewidth narrowing of a DL above threshold will be subjects of further theoretical research elsewhere. DL arrays are expected to act as sources of radiation, coherent in space and time, providing an alternative to conventional lasers. One of the advantages of DL arrays is that they do not need an optical cavity. Another advantage is that they can be flexibly arranged in various planar or three-dimensional spatial structures to form radiation patterns with a similar principle of operation as for phased dipole arrays in radio physics. The second-order DL phase transition corresponds to a singularity in the polarizability of the particles, similar to the lasing phase transition, which corresponds to a singularity in the amplification coefficient of a linear amplifier with an optical cavity [31]. We have presented an analysis of such singularities and proposed a route to the calculation of other DL parameters such as the radiation rate. The analysis can be applied to other nanoobjects or heterogeneous media where the local field and optical amplification lead to singularities in the polarizability. These could include, for example, a single metal nanoparticle in the amplified medium [16,18] or a nanoparticle with a metal core and an optically active shell. When an external field is applied in the DL regime, the radiation rate is predicted to exhibit a strongly nonlinear, multistable behavior, undergoing a first-order phase transition as a function of applied field intensity, even if the field intensity may be very small. This suggests the use of nanoparticles operating in the DL regime as sensors to amplify weak optical signals. The identification of regions of parameter space where bistability can be demonstrated in a DL can be carried out using standard methods of catastrophe theory.

We propose that metal nanoparticles on the surface of a semiconductor substrate with a radiative *p-n* junction provide a relatively easy scheme for the experimental realization and investigation of DL. Initial experiments should demonstrate an enhancement of electroluminescence due to the nanoparticles. The LPR needs to be matched with the maximum amplification in the substrate. Then, at a pump rate providing sufficient population inversion in the substrate, one can search for a nonlinear dependence of electroluminescence on the pump rate and, finally, for a DNL phase transition.

In principle, such a system can also operate in a reverse way to a DL, i.e., by absorbing external radiation and generating a photocurrent, thus providing an efficient approach to photovoltaics [40,10].

The DL phase transition resembles the ferroelectric phase transition in a constant electric field [26]; the DL medium is essentially a ferroelectric medium in the optical domain. A key difference between the DL and a conventional ferroelectric is that optical losses are inevitable in the DL medium, while such losses are not present in a ferroelectric in a constant electric field. The DL phase transition can be realized in a medium with optical gain to compensate the losses. In contrast to conventional ferroelectric media, a DL medium may be constructed artificially by placing metal particles and active light emitters into the dielectric matrix. In this way, optical properties of the DL medium, such as the resonance frequency and the radiation pattern, may be controlled. Coherent radiation in the DL regime is then of interest for a wide range of phenomena including, for example, super-radiance from an ensemble of dipole nanolasers.

ACKNOWLEDGMENTS

We thank Science Foundation Ireland and Enterprise Ireland International Collaboration Program 2005 for supporting this work.

[1] N. Félidj, J. Aubard, G. Lévi, J. R. Krenn, M. Salerno, G. Schider, B. Lamprecht, A. Leitner, and F. R. Aussenegg, Phys. Rev. B **65**, 075419 (2002).
[2] O. G. Tovmachenko, C. Graf, D. J. van den Heuvel, A. van Blaaderen, and H. C. Gerritsen, Adv. Mater. (Weinheim, Ger.) **18**(1), 91 (2006).
[3] J. C. G de Sande, R. Serna, J. Gonzalo, C. N. Afonso, and D. H. Hole, J. Appl. Phys. **91**, 1536 (2002).
[4] E. M. Hicks, S. Zou, G. C. Schatz, K. G. Spears, R. P. Van Duyne, L. Gunnarsson, T. Rindzevicius, B. Kasemo, and M. Käll, Nano Lett. **5**, 1065 (2005).
[5] M. Moskovitch, Rev. Mod. Phys. **57**, 783 (1985); J. J. Mock, M. Barbic, D. R. Smith, D. A. Schultz, and S. Schultz, J. Chem. Phys. **116**(15), 6755 (2002).
[6] Surface plasmon resonance biosensors are manufactured, for example, by Thermo Labsystems Affinity Sensors Division, Saxon Way Bar Hill Cambridge CB3 8SL, UK.
[7] K. Kurihara, T. Arai, T. Nakano, and J. Tominaga, Jpn. J. Appl. Phys., Part 1 **44**, 3353 (2005).
[8] V. V. Klimov, JETP Lett. **78**, 471 (2003).
[9] B. P. Rand, P. Peumans, and S. R. Forrest, J. Appl. Phys. **96**, 7519 (2004).
[10] I. E. Protsenko, N. F. Starodubtsev, V. M. Rudoy, O. V. Dement'eva, N. V. Naumov, O. A. Zaimidoroga, and V. N. Samoilov, Reports of RAS, Physic **70**, 510 (2006).
[11] S. A. Maier, Current Nanoscience **1**(1), 17 (2005).
[12] O. A. Zajmidoroga, I. E. Protsenko, and V. N. Samojlov, Russian Federation Patent No. 2003111147/28 (April 21, 2003).
[13] I. E. Protsenko, A. V. Uskov, O. A. Zaimidoroga, V. N. Samoilov, and E. P. O'Reilly, Phys. Rev. A **71**, 063812 (2005).
[14] D. J. Bergman and M. I. Stockman, Phys. Rev. Lett. **90**, 027402 (2003).
[15] C. J. Bottcher, *Theory of Electric Polarization: Dielectrics in Static Fields*, 1st reprint (Elsevier Science Pub. Co., New York, 1993).
[16] A. N. Oraevskii and I. E. Protsenko, JETP Lett. **72**(9), 445 (2000).
[17] A. N. Oraevskij and I. E. Protsenko, Russian Federation Patent No. 2001104305/28 (16 February 2001).
[18] N. M. Lawandy, Appl. Phys. Lett. **85**, 5040 (2004).
[19] H. A. Lorentz, Wiedem. Ann. **9**, 641 (1880); **11**, 70 (1881).
[20] A. V. Ghiner and G. I. Surdutovich, Phys. Rev. A **49**, 1313 (1994).
[21] J. A. Leegwater and S. Mukamel, Phys. Rev. A **49**, 146 (1994).
[22] M. G. Benedict, V. A. Malyshev, E. D. Trifonov, and A. I. Zaitsev, Phys. Rev. A **43**, 3845 (1991).
[23] C. M. Bowden and J. P. Dowling, Phys. Rev. A **47**, 1247 (1993).
[24] J. P. Dowling and C. M. Bowden, Phys. Rev. Lett. **70**, 1421 (1993).
[25] J. D. Jackson, *Classical Electrodynamics* (Wiley, New York, 1975).
[26] Charles Kittel, *Introduction to Solid State Physics*, 8th ed. (John Wiley & Sons, New York, 2004), p. 453.
[27] E. M. Lifshitz, L. D. Landau, and L. P. Pitaevskii, *Electrodynamics of Continuous Media*, Vol. 8: Course of Theoretical Physics, 2nd ed. (Butterworth-Heinemann, Washington, DC, 1984), pp. 77–85.
[28] V. A. Sautenkov, H. van Kampen, E. R. Eliel, and J. P. Woerdman, Phys. Rev. Lett. **77**, 3327 (1996).
[29] A. Z. Genack and J. M. Drake, Nature **368**, 400 (1994).
[30] I. Protsenko, P. Domokos, V. Lefèvre-Seguin, J. Hare, J. M. Raimond, and L. Davidovich, Phys. Rev. A **59**, 1667 (1999).
[31] J. Jahanpanah and R. Loudon, Phys. Rev. A **56**, 2255 (1997).
[32] M. Sargent III, M. O. Scully, and W. E. Lamb Jr., *Laser Physics* (Addison-Wesley, Reading, MA, 1974).
[33] T. Poston and I. Stewart, *Catastrophe Theory and Its Applications* (Dover Publications, New York, 1996).
[34] R. Hillenbrand, T. Taubner, and F. Keilmann, Nature **418**, 159 (2002).
[35] E. D. Palik and G. Ghosh, *Handbook of Optical Constants of Solids* (Academic Press, New York, 1985).
[36] J. C. Maxwell-Garnett, Philos. Trans. R. Soc. London **203**, 385 (1904); **205**, 327 (1906).
[37] S. M. Kachan and A. N. Ponyavina, J. Mol. Struct. **563**, 267 (2001).
[38] I. E. Protsenko, JETP **102**, 167 (2006).
[39] W. L. Stutzman and G. A. Thiele, *Antenna Theory and Design*, 2nd ed. (Wiley, New York, 1997).
[40] B. P. Rand, P. Peumans, and S. R. Forrest, J. Appl. Phys. **96**, 7519 (2004).